The Laplace Tidal Equations and Atmospheric Tides

David A. Randall

Department of Atmospheric Science
Colorado State University, Fort Collins, Colorado 80523

34.1 Free and forced small-amplitude oscillations of a thin spherical atmosphere

34.1.1)Perturbation equations

Laplace (originally published in French in 1799; English translation in 1832) was the first to investigate the free and forced oscillations of a thin atmosphere on a spherical planet. His 200-year old paper is still very relevant today.

The basic state considered by Laplace has a highly idealized form:

$$\overline{V}_h = 0, \overline{\omega} = 0, \frac{\partial\overline{\phi}}{\partial p} = -\overline{\alpha}, p\overline{\alpha} = R\overline{T}(p). \tag{34.1}$$

here $T(p)$ is an arbitrary function of p. Note that T does *not* depend on latitude. This state has no meridional temperature gradient and no mean flow. It is, of course, in balance.

The linearized governing equations are

$$\frac{\partial u'}{\partial t} = (2\Omega\sin\varphi)v' - \frac{1}{a\cos\varphi}\frac{\partial\phi'}{\partial\lambda}, \tag{34.2}$$

$$\frac{\partial v'}{\partial t} = -(2\Omega\sin\varphi)u' - \frac{1}{a}\frac{\partial\phi'}{\partial\varphi}, \tag{34.3}$$

$$\frac{1}{a\cos\varphi}\left[\frac{\partial u'}{\partial\lambda} + \frac{\partial}{\partial\varphi}(v'\cos\varphi)\right] + \frac{\partial\omega'}{\partial p} = 0, \tag{34.4}$$

$$\frac{\partial}{\partial p}\left(\frac{\partial\phi'}{\partial t}\right) + S_p\omega' = -\frac{R}{c_p}\frac{Q}{p}, \tag{34.5}$$

where $S_p \equiv -\frac{\overline{\alpha}}{\overline{\theta}}\frac{\partial\overline{\theta}}{\partial p}$ is the static stability, which depends on p, and Q is the heating. Friction has been neglected. Also,

$$\phi' = gz' + \Phi(\lambda, \varphi, t) , \tag{34.6}$$

where Φ is the *external* gravitational tidal potential, due to the moon and/or sun. In (34.6), we recognize that the atmosphere experiences gravitational accelerations due to the pulls of the moon and sun, in addition to that of the Earth. The variation of Φ with p is negligible, because the atmosphere is thin compared to the distances to the sun and moon. Note that these equations are valid only for atmospheres which are shallow compared to the planetary radius, a.

We look for solutions of the form

$$\begin{bmatrix} u' \\ v' \\ \omega' \\ \phi' \\ Q \end{bmatrix} = \begin{bmatrix} u^{\sigma, s}(\varphi, p) \\ v^{\sigma, s}(\varphi, p) \\ \omega^{\sigma, s}(\varphi, p) \\ \phi^{\sigma, s}(\varphi, p) \\ Q^{\sigma, s}(\varphi, p) \end{bmatrix} exp[i \underbrace{(s\lambda + \sigma t)}_{phase}] , \tag{34.7}$$

where

$$s = \text{zonal wave number} = 0, 1, 2\ldots$$

$$\sigma = \text{frequency}, \sigma < 0 \rightarrow \text{eastward moving}$$

$$\sigma > 0 \rightarrow \text{westward moving} .$$

The superscripts σ, s simply denote the particular frequency and zonal wave number associated with each mode. Using $\frac{\partial}{\partial t} = i\sigma$, and $\frac{\partial}{\partial \lambda} = is$, we see that (34.2) and (34.3) can be written as

$$i\sigma u^{\sigma, s} = (2\Omega \sin\varphi) v^{\sigma, s} - \frac{is}{a\cos\varphi}\phi^{\sigma, s} , \tag{34.8}$$

$$i\sigma v^{\sigma, s} = -(2\Omega \sin\varphi) u^{\sigma, s} - \frac{1}{a}\frac{\partial \phi^{\sigma, s}}{\partial \varphi} . \tag{34.9}$$

Solving for $u^{\sigma, s}$ and $v^{\sigma, s}$, we find that

$$u^{\sigma, s} = \frac{1}{2\Omega(\nu^2 - \sin^2\varphi)}\left(\sin\varphi\frac{\partial}{\partial\varphi} - \frac{\nu s}{\cos\varphi}\right)\frac{\phi^{\sigma, s}}{a} , \tag{34.10}$$

$$v^{\sigma,s} = \frac{i}{2\Omega(\nu^2 - \sin^2\varphi)}\left(\nu\frac{\partial}{\partial\varphi} - s\tan\varphi\right)\frac{\phi}{a} , \tag{34.11}$$

where $\nu \equiv \frac{\sigma}{2\Omega}$ is the *normalized* frequency. Substituting (34.10) and (34.11) into the continuity equation (34.4) gives

$$\frac{i}{2\Omega a^2}\left\{\frac{s}{(\nu^2 - \sin^2\varphi)}\left(\frac{\sin\varphi}{\cos\varphi}\frac{\partial}{\partial\varphi} - \frac{\nu s}{\cos^2\varphi}\right) + \right.$$

$$\left.\frac{1}{\cos\varphi}\frac{\partial}{\partial\varphi}\left[\frac{1}{(\nu^2 - \sin^2\varphi)}\left(\frac{\nu\cos^2\varphi}{\cos\varphi}\frac{\partial}{\partial\varphi} - s\sin\varphi\right)\right]\right\}\phi^{\sigma,s} + \frac{\partial\omega^{\sigma,s}}{\partial p} = 0 . \tag{34.12}$$

Now introduce a new "latitude" variable, $\mu \equiv \sin\varphi$. This change of variables is useful because of the convergence of the meridians. Note that $d\mu \equiv \cos\varphi d\varphi$. Then from (34.12) and (34.5) we get two equations for the two unknowns $\phi^{\sigma,s}$ and $\omega^{\sigma,s}$:

$$\frac{i\sigma}{4a^2\Omega^2}F(\phi^{\sigma,s}) + \frac{\partial\omega^{\sigma,s}}{\partial p} = 0 , \tag{34.13}$$

$$i\sigma\frac{\partial\phi^{\sigma,s}}{\partial p} + S_p\omega^{\sigma,s} = -\frac{R}{c_p}\frac{Q^{\sigma,s}}{p} . \tag{34.14}$$

Here F is an operator that involves μ, s, and ν:

$$F \equiv \frac{\partial}{\partial\mu}\left(\frac{1-\mu^2}{\nu^2-\mu^2}\frac{\partial}{\partial\mu}\right) - \frac{1}{(\nu^2-\mu^2)}\left[\frac{s}{\nu}\left(\frac{\nu^2+\mu^2}{\nu^2-\mu^2}\right) + \frac{s^2}{1-\mu^2}\right] . \tag{34.15}$$

Some algebra is needed to obtain this form of F. Eliminating $\phi^{\sigma,s}$ between (34.13) and (34.14) gives

$$4\Omega^2 a^2\frac{\partial^2\omega^{\sigma,s}}{\partial p^2} - S_p(p)F(\omega^{\sigma,s}) = \frac{R}{c_p}\frac{F(Q^{\sigma,s})}{p} . \tag{34.16}$$

For now we regard $Q^{\sigma,s}$ as known, so that (34.16) contains the single unknown $\omega^{\sigma,s}(\varphi,p)$. The assumption that $Q^{\sigma,s}$ is known means that $Q^{\sigma,s}$ is at least approximately independent of the motion. An example would be heating due to absorption of solar radiation by ozone.

You are strongly encouraged to work through the details of the derivation from the beginning of this section up to (34.16).

A further separation of variables (see box) is achieved by assuming that for a given pair (σ, s) ,

$$\begin{aligned}\phi^{\sigma, s} &= \sum_n Z_n^{\sigma, s}(p)\Theta_n^{\sigma, s}(\varphi) , \\ \omega^{\sigma, s} &= \sum_n W_n^{\sigma, s}(p)\Theta_n^{\sigma, s}(\varphi) , \\ Q^{\sigma, s} &= \sum_n J_n^{\sigma, s}(p)\Theta_n^{\sigma, s}(\varphi) .\end{aligned} \tag{34.17}$$

Here the subscript n is introduced to recognize the possibility of multiple solutions, and the summation over n just represents superposition of these solutions. It can be shown that the set $\{\Theta_n^{\sigma, s}(\varphi)\}$ for all n is *complete* for $-\frac{\pi}{2} \le \varphi \le \frac{\pi}{2}$. At this point, we do not know what the meridional structure represented by $\Theta_n^{\sigma s}(\varphi)$ is. Substitution of (34.17) into (34.16) gives:

$$F(\Theta_n^{\sigma, s}) = -\varepsilon_n \Theta_n^{\sigma, s} , \tag{34.18}$$

$$\frac{d^2 W_n^{\sigma, s}}{dp^2} + \frac{S_p}{gh_n} W_n^{\sigma, s} = -\frac{R}{gh_n c_p}\left(\frac{J_n^{\sigma, s}}{p}\right) . \tag{34.19}$$

Here we have introduced the nondimensional quantity

$$\varepsilon_n \equiv \frac{4\Omega^2 a^2}{gh_n} \tag{34.20}$$

The quantity h_n, which appears in (34.19) and (34.20), is the "separation constant." It is called the "equivalent depth," for reasons that will become clear later.

For reasons that should be obvious, Eq. (34.18) is called the meridional structure equation, and Eq. (34.19) is called the vertical structure equation. Recall that we have derived these equations using the assumption that the basic state is at rest, and that the temperature depends on pressure (i.e. height) only. Separation of variables becomes impossible if the basic state is made more realistic, e.g. if the observed zonally averaged temperature and winds are used.

Separation of Variables

The motion of a vibrating string is described by

$$\frac{\partial^2 u}{\partial t^2} = a^2 \frac{\partial^2 u}{\partial x^2} .$$

Assume a solution of the form

$$u(x, t) = X(x) \cdot T(t) . \quad ,$$

i.e. a function of x only multiplied by a function of t only. Then substitution gives

$$XT'' = a^2 X'' T ,$$

which can be written as

$$\frac{X''}{X} = \frac{T''}{a^2 T} .$$

Since X is independent of t, and T is independent of x, we conclude that

$$\frac{X''}{X} = \lambda , \text{ and } \frac{T''}{a^2 T} = \lambda ,$$

Eq. (34.18) was derived by Laplace about 200 years ago. It is often called the Laplace Tidal Equation or LTE. Using the definition of F, we can expand the LTE into the alternative form

$$\frac{d}{d\mu}\left[\left(\frac{1-\mu^2}{\nu^2-\mu^2}\right)\frac{d\Theta^{\sigma, s}{}_n}{d\mu}\right] - \frac{1}{(\nu^2-\mu^2)}\left[\frac{s}{\nu}\left(\frac{\nu^2+\mu^2}{\nu^2-\mu^2}\right) + \frac{s^2}{1-\mu^2}\right]\Theta_n^{\sigma, s} + \varepsilon_n \Theta_n^{\sigma, s} = 0 . \quad (34.21)$$

The LTE is a second-order ordinary differential equation and so it requires two boundary conditions. It suffices to assume that the $\Theta_n^{\sigma, s}$ must be bounded at the poles, i.e. at $\mu = -1$ and 1 .

Note that (34.21) and its boundary conditions are satisfied quite nicely by the trivial solution $\Theta_n^{\sigma, s} = 0$. Non-trivial solutions do exist, but only for particular choices of the parameters ν and/or h_n (or ε_n). If these parameters are chosen "at random," the *only* solution of (34.18) that satisfies the boundary conditions is the trivial solution $\Theta_n^{\sigma, s} = 0$. A problem of this type is called an "eigenvalue problem." The frequencies and/or equivalent depths are the eigenvalues and the $\Theta_n^{\sigma, s}$ are the eigenfunctions or eigenvectors, which are called *Hough functions*.

Note that all information about the planetary radius, rotation rate, and gravity is "buried" in ε_n and ν. The parameter ε_n is sometimes given the imposing name "the terrestrial constant." Because it contains only two non-dimensional parameters characterizing the planet, the LTE does not "know" or "care" very much about the particular planet to which it is being applied. For given s, ν, and ε_n, the eigenvalues and eigenfunctions of (34.21) are the same for all planets, provided that the atmosphere in question is shallow compared to the planetary radius. This means that the solutions of (34.21) have a very broad applicability.

The LTE itself describes only the meridional structure of the oscillations. It could be called the "meridional structure equation." The vertical structure of the solution is governed by (34.19), which, naturally enough, is called the "*vertical structure equation*." It is a second-order ordinary differential equation for $W_n^{\sigma, s}(p)$. At the top of the atmosphere we apply the boundary condition

$$W_n^{\sigma, s} = 0 \text{ at } p = 0 . \tag{34.22}$$

This is exact.

At the lower boundary, the exact boundary condition (in the absence of mountains) is $w \equiv \frac{Dz}{Dt} = 0$ at $p = p_S$. We apply the linearized boundary condition

$$\frac{Dz}{Dt} \cong \left(\frac{\partial z'}{\partial t}\right)_p + \omega' \frac{\partial \bar{z}}{\partial p} = 0 \text{ at } p = p_0 . \tag{34.23}$$

Here p_0 is the value of p_S in the basic state. Because

$$gz' = \phi' - \Phi , \tag{34.24}$$

where $\Phi(\lambda, \varphi, t)$ is known, and using the hydrostaticity of the basic state, as expressed by

$$g\left(\frac{\partial \bar{z}}{\partial p}\right)_{p = p_0} = -\bar{\alpha}_0 = -\frac{R\bar{T}_0}{p_o} , \tag{34.25}$$

we can rewrite the lower boundary condition (34.23) as

$$\frac{\partial \phi'}{\partial t} - \omega' \frac{R\overline{T}_0}{p_0} = \frac{\partial \Phi}{\partial t} \text{ at } p = p_0 , \tag{34.26}$$

or

$$i\sigma\phi - \frac{R\overline{T}_0}{p_o}\omega = i\sigma\Phi \text{ at } p = p_0 . \tag{34.27}$$

(Note that we retain the symbol Φ here for notational simplicity.) The tidal forcing thus enters through the lower boundary condition.

Eliminating ϕ between (34.27) and (34.13) (as applied at $p = p_0$) gives

$$\frac{\partial \omega}{\partial p} + \frac{1}{4\Omega^2 a^2}\frac{R\overline{T}_0}{p_0}F(\omega) = -\frac{i\sigma}{4\Omega^2 a^2}F(\Phi) \text{ at } p = p_0 . \tag{34.28}$$

Expressing Φ in terms of Hough functions, i.e.

$$\Phi = \sum_n G_n \Theta_n(\varphi) , \tag{34.29}$$

we finally obtain the lower boundary condition as

$$\frac{dW_n}{dp} - \frac{R\overline{T}_0}{p_0 g h_n} W_n = \frac{i\sigma}{g h_n} G_n \text{ at } p = p_0 . \tag{34.30}$$

Note that the gravitational forcing enters the problem through the lower boundary condition on the vertical structure equation. The thermal forcing enters through the vertical structure equation itself. The gravitational and thermal forcings do not appear in the LTE.

34.1.2)Free oscillations of the first and second kinds

A free oscillation is one for which there is no thermal or gravitational forcing. When there is *no thermal forcing* the vertical structure equation (34.19) reduces to

$$\frac{d^2 W}{dp^2} + \frac{S_p}{gh} W = 0 . \tag{34.31}$$

When there is *no gravitation forcing* the surface boundary condition (34.30) can be simplified to

$$\frac{dW}{dp} - \frac{R\overline{T}_0}{ghp_0}W = 0 \ \text{ at } \ p = p_0 \, . \tag{34.32}$$

We also have

$$W = 0 \text{ at } p = 0 \, . \tag{34.33}$$

Then (34.31) has non-trivial solutions only for special values of h. These eigenvalues are denoted by $\hat{h}$. For $h \neq \hat{h}$, only the trivial solution [i.e. $W_n(p) \equiv 0$] exists. In order to find the $\hat{h}$ and the corresponding solutions for $W_n(p)$, we have to specify the static stability S_p as a function of height. Different choices for S_p will give different h_n and $W_n(p)$.

For the case of free oscillations, the solution procedure is shown in Fig. 34.1. Note that in this case we have *two* eigenvalue problems: One from the vertical structure

(34.31), (34.32), and (34.33), for given $S_p(p)$ $\longrightarrow$ possibly infinite set of h_n and $W_n(p)$ $\xrightarrow{(34.21)}$ $\Theta_n^{\sigma,\, s}$ and $\sigma(s, n)$

Figure 34.1: The solution procedure for free oscillations. The vertical structure equation is solved first. The frequency is obtained as an eigenvalue of the LTE.

equation, and a second from the LTE. In the vertical structure problem, the eigenvalues are the equivalent depths. In the meridional structure problem, the eigenvalues are the frequencies.

As a very simple example, suppose that the atmosphere is isentropic, so that $S_p = 0$. Then we find from (34.31) that

$$\frac{d^2W}{dp^2} = 0 \, . \tag{34.34}$$

A solution of (34.34) that is consistent with the upper boundary condition (34.33) is

$$W = Ap \, , \tag{34.35}$$

where A is an arbitrary constant. Use of (34.35) in the lower boundary condition (34.32) gives

$$\hat{h} = \frac{R\overline{T}_0}{g} \equiv H_0 . \tag{34.36}$$

This is the only possible equivalent depth for free oscillations of an isentropic atmosphere. *With more general stratifications there can be many (infinitely many) equivalent depths.* The basic procedure used in this simple example would be the same for other stratifications.

With $\hat{h}$ given by (34.36), nontrivial solutions of (34.18) exist only when there is a special relation (called the dispersion relation) among ν, s, and n. We refer to n as the "wave type." The Hough functions [i.e. the solutions of (34.18)] have been tabulated by Longuet-Higgins (1968) and others. Here we consider only some limiting cases. First suppose that there is no rotation, so that $\nu = \frac{\sigma}{2\Omega} \to \infty$. We continue to assume that $S_p = 0$ so that (34.36) applies. For this case, find that

$$\nu^2 F \to \frac{d}{d\mu}\left[(1-\mu^2)\frac{d}{d\mu}\right] - \frac{s^2}{1-\mu^2} , \tag{34.37}$$

and

$$\nu^2 \varepsilon \to \frac{\sigma^2 a^2}{g\hat{h}} = \frac{\sigma^2 a^2}{gH_0} . \tag{34.38}$$

Then the LTE, (34.21), reduces to

$$\frac{d}{d\mu}\left[(1-\mu^2)\frac{d\Theta}{d\mu}\right] + \left(\frac{\sigma^2 a^2}{gH_0} - \frac{s^2}{1-\mu^2}\right)\Theta = 0 . \tag{34.39}$$

It can be shown that (34.39) has solutions that are bounded as $\mu \to \pm 1$ *only for*

$$\frac{\sigma^2 a^2}{gH_0} = n(n+1), n = 1, 2, 3\ldots \tag{34.40}$$

These are eigenvalues again. Think of (34.40) as fixing the allowed frequencies of the waves. The eigenfunctions are called associated Legendre Functions of order n and rank s, denoted by

$$\Theta_n = P_n^s(\mu) \qquad (n \geq s) . \tag{34.41}$$

Note that n and s are both integers such that $n \geq s$. When combined with the longitudinal factor, we find that the latitude-longitude structure of the waves is

$$Y_n^s(\mu, \lambda) = P_n^s(\mu) exp(is\lambda) . \tag{34.42}$$

These are the spherical harmonics (see the handout on this topic). Here n is the total number of nodal circles, s is the zonal wave number, and n-s is the number of nodes in the meridional direction, also known as the "meridional nodal number."

The solutions found here are external gravity waves. They are called "external" because they have no nodes in the vertical. The frequency

$$\sigma = \pm\frac{\sqrt{n(n+1)gH_0}}{a} \tag{34.43}$$

depends on the wave's scale through the two-dimensional index, n, but it *is independent of* s. For example, when $n = 1$, s can be either 0 or 1, but both modes have the same frequency. This is not true when rotation is present, because then the zonal direction (in which scale is measured by s) becomes physically "different" from the meridional direction. A non-isentropic atmosphere can support both external and internal gravity waves.

Now we consider $\Omega \neq 0$, still for an isentropic atmosphere, and neglect all details. Define a stream function ψ and a velocity potential χ so that

$$\begin{aligned} u' &= -\frac{1}{a}\left(\frac{\partial\psi}{\partial\varphi}\right)_p + \frac{1}{a\cos\varphi}\left(\frac{\partial\chi}{\partial\lambda}\right)_p \\ v' &= \frac{1}{a\cos\varphi}\left(\frac{\partial\psi}{\partial\lambda}\right)_p + \frac{1}{a}\left(\frac{\partial\chi}{\partial\varphi}\right)_p \end{aligned} . \tag{34.44}$$

The vorticity is then $\xi_p = \boldsymbol{k} \cdot (\nabla_p \times \boldsymbol{V}_h) = \nabla_p^2\psi$, and the divergence is $\delta_p = \nabla_p \cdot \boldsymbol{V}_h = \nabla_p^2\chi$. The equation of horizontal motion leads to

$$\frac{\partial}{\partial t}\nabla_p^2\psi + \frac{2\Omega\cos\varphi}{a}v' + 2\Omega\sin\varphi \cdot \nabla_p^2\chi = 0 \tag{34.45}$$

(the vorticity equation) and

$$\frac{\partial}{\partial t}\nabla_p^2\chi + \frac{2\Omega\cos\varphi}{a}u' - 2\Omega\sin\varphi \cdot \nabla_p^2\psi = -g\nabla_p^2 z' \tag{34.46}$$

(the divergence equation). We can also show (see the problems at the end of this chapter) that

$$\frac{\partial z'}{\partial t} + H_0\nabla_p^2\chi = 0 . \tag{34.47}$$

Equations (34.44) through (34.47) form a closed set that can be solved for ψ, χ, and z'.

From (34.45) and (34.47) we see that stationary motion cannot exist unless $v' = 0$. For nontrivial stationary motion with $v' = 0$ it follows from (34.2) that $s = 0$, i.e. the motion must be purely zonal and also zonally uniform.

Margules (1893) and Hough (1898) showed that the LTE has two classes of solutions, which they named Free Oscillations of the First and Second Classes. For the case of $\varepsilon \equiv \frac{4\Omega^2 a^2}{g\hat{h}}$ small (weak rotation), we can solve (34.45) and (34.46) by expanding in spherical harmonics (see Longuet-Higgins, 1968). The Free Oscillations of the First Class (FOFC) are essentially gravity waves, satisfying

$$\left.\begin{aligned} \chi &\cong A_n^s P_n^2(\mu) e^{i(s\lambda + \sigma t)} \\ \psi &\cong 0 \ \ (\text{irrotational}) \\ \sigma^2 &\cong \frac{gH_0}{a^2} n(n+1) \end{aligned}\right\} . \tag{34.48}$$

Compare with our earlier results, obtained for $\Omega = 0$. Haurwitz (1937) obtained a more accurate expression for the frequency of the FOFC:

$$\sigma \cong \frac{\Omega s}{n(n+1)} \pm \sqrt{\frac{\Omega^2 s^2}{n^2 (n+1)^2} + n(n+1)\frac{gH_0}{a^2}} . \tag{34.49}$$

This should be compared with (34.48). The additional terms in (34.49) involve Ω. For $n \ge 4$ the error in (34.49) is less than 1%. From (34.49) we see that eastward propagating inertia gravity waves have frequencies slightly different from those of westward propagating inertia gravity waves. The difference is due to rotation.

The Free Oscillations of the Second Kind (FOSC) are the so-called Rossby-Haurwitz waves, which satisfy

$$\left.\begin{aligned} \psi &\cong iB_n^s P_n^2(\mu) e^{i(s\lambda + \sigma t)} \\ \chi &\cong 0 \ \ (\text{nondivergent}) \\ \sigma &\cong \frac{2\Omega s}{n(n+1)} > 0 \end{aligned}\right\} . \tag{34.50}$$

Note that, since $\sigma > 0$, *the FOSC always move westward*. They are nearly nondivergent. They can be found by assuming $\chi = 0$ from the beginning, as follows: The linearized nondivergent vorticity equation is

$$\frac{\partial}{\partial t}\nabla^2\psi + \frac{2\Omega}{a^2}\frac{\partial\psi}{\partial\lambda} = 0 . \tag{34.51}$$

Therefore

$$i\sigma\left\{\frac{1}{a^2\cos^2\varphi}\left[\cos\varphi\frac{d}{d\varphi}\left(\cos\varphi\frac{d\hat{\psi}}{\partial\varphi}\right) - s^2\hat{\psi}\right]\right\} + \frac{2\Omega i s}{a^2}\hat{\psi} = 0 , \tag{34.52}$$

or

$$\frac{d}{d\mu}\left[(1-\mu^2)\frac{d\hat{\psi}}{d\mu}\right] + \left(\frac{2\Omega s}{\sigma} - \frac{s^2}{1-\mu^2}\right)\hat{\psi} = 0 . \tag{34.53}$$

This is another eigenvalue problem. The solution of (34.53) is $\hat{\psi} = B_n^s P_n^s(\mu)$, so that

$$\left.\begin{aligned}\psi &= B_n^s P_n^s e^{i(s\lambda + \sigma t)} \\ \sigma &= \frac{2\Omega s}{n(n+1)}\end{aligned}\right\} . \tag{34.54}$$

Note that for these waves, unlike the pure gravity waves, σ does depend explicitly on *s*.

This westward propagation of Rossby-Haurwitz waves is due to the Earth's sphericity. To see this, rewrite (34.51) as

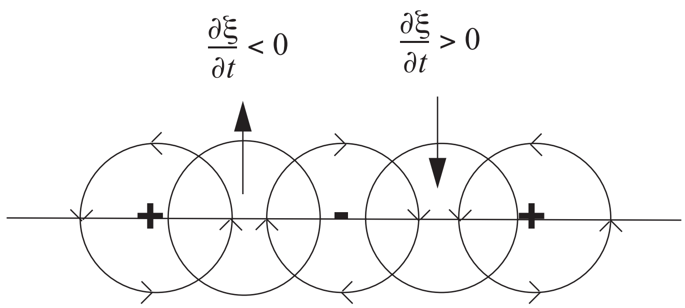

Figure 34.2: Chain of vortices along a latitude circle, illustrating the westward propagation of Rossby waves.

$$\frac{\partial}{\partial t}\xi + \beta v = 0 , \tag{34.55}$$

where

$$\beta \equiv \frac{2\Omega\cos\varphi}{a} = \frac{1}{a}\frac{df}{d\varphi} . \tag{34.56}$$

Note that $\beta \geq 0$. Consider a chain of vortices along a latitude circle, as shown in Fig. 34.2. In places where $v > 0$, $\beta v > 0$, so $\frac{\partial\xi}{\partial t} < 0$. Similarly, where $v < 0$, $\beta v < 0$, so $\frac{\partial\xi}{\partial t} > 0$.

A direct test of the theory of non-divergent Rossby waves was made by Eliassen and Machenhauer (1965) and Deland (1965). They performed a spherical-harmonic analysis of the 500 mb stream function, isolating transient waves by taking the difference in 24 hours. Their results, illustrated in Fig. 34.3, show westward propagation. Table 34.1

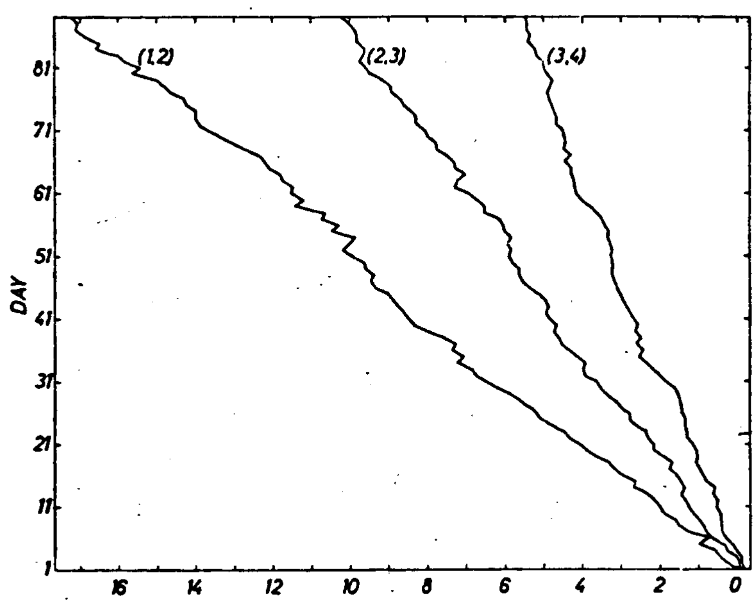

Figure 34.3: Successive daily values of the phase angle for the 24 hour tendency field, $\psi_{s,n}(l+1) - \psi_{s,n}(t)$, at the 500 mb level for the components $(s, n) = (1, 2), (2, 3), (3, 4)$, during the 90 day period beginning 1 December 1956. The abscissa represents the number of westward circulations round the Earth after the first passage of the Greenwich meridian. From Eliassen and Machenhauer (1965).

compares the computed [from (34.54)] and observed phase speeds, in degrees of longitude per day.The model overpredicts the westward phase speeds. This error is due to our neglect of the effects of divergence.

Madden and Julian (1972) found a 5-day oscillation of surface pressure in the tropics, which corresponds to a FOSC with $n = 2$, $s = 1$. It drifts westward, as shown in Fig. 34.4.

Table 34.2 gives examples of the periods of the FOFC and FOSC. Notice that

(s, n)	$c_{R\text{-}H}$	c_{obs}
(1,2)	-115	-70
(2,3)	-53	-40
(3,4), (1,4)	-28	-20
(2,5)	-16	-12
(3,6)	-9	-8

Table 34.1: Predicted and observed phase speeds of Rossby-Haurwitz modes, in degrees of longitude per day.

westward moving gravity waves with $n = 2$, $s = 2$ have periods close to 12 hours. These modes are observed, and early theories attributed their period to semidiurnal forcing. This point is discussed further later.

34.2 Atmospheric Tides

The atmospheric tides were first detected as small amplitude, large-scale surface pressure oscillations with periods that divide evenly into a day; see Fig. 34.5. At the surface, the *semidiurnal* solar barometric tide is the most prominent. Its existence is easily detected at tropical stations. In higher latitudes the barometric tide is weaker, and also the day-to-day synoptic fluctuations of surface pressure are stronger, so the tides are less conspicuous.

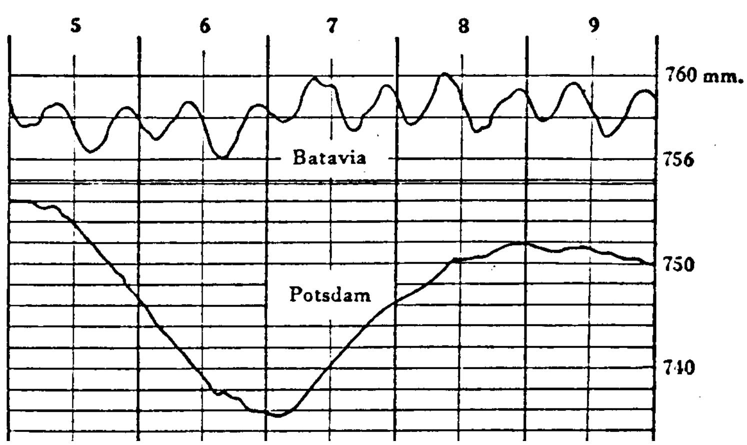

Figure 34.5: A barometric record taken at a tropical station, together with one taken in a temperature latitude. The horizontal axis is time in days.

The various tides are denoted by S_l and L_l for solar and lunar modes,

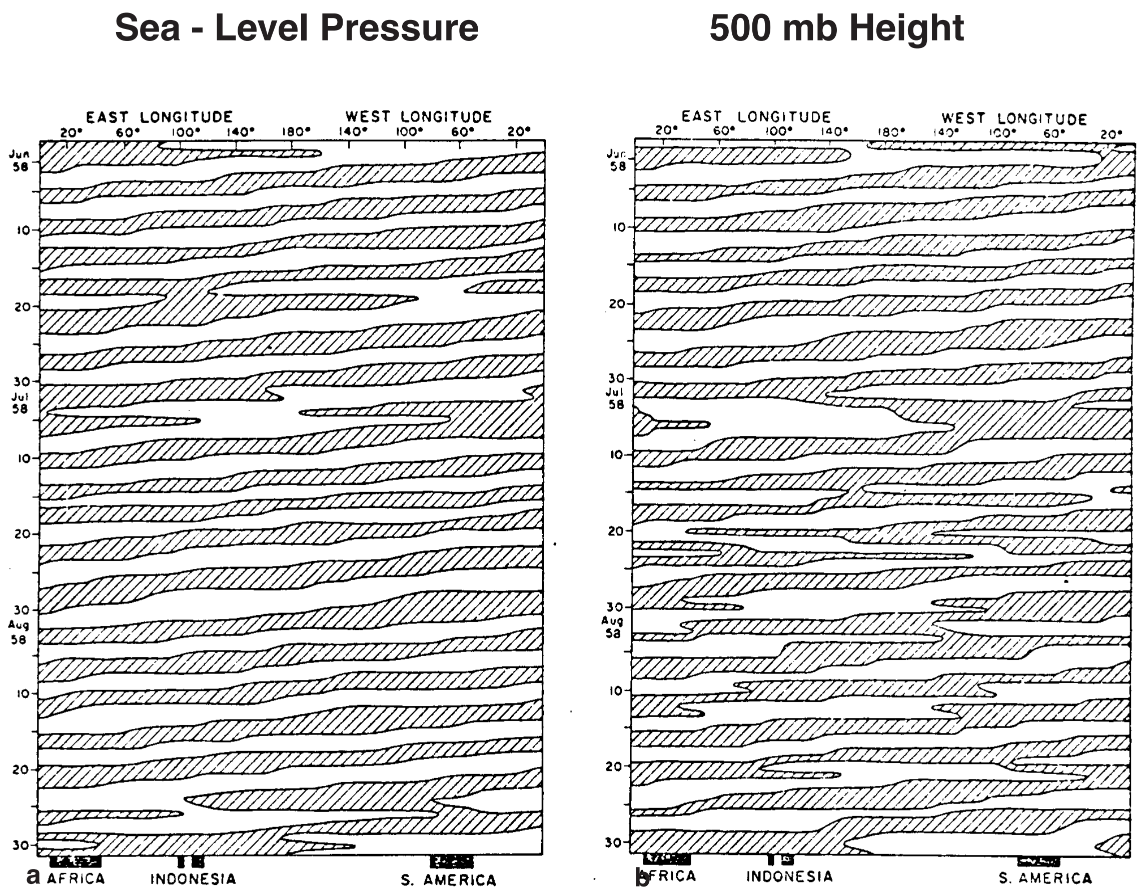

Figure 34.4: a) Longitude-time diagrams of zonal wavenumber 1 anomalies of the high-pass filtered sea-level pressures. b) 500-mb heights from 25S to 25N. Shaded areas represent negative anomalies. From Madden and Julian (1972).

respectively. Here S_l is the l^{-1} diurnal oscillation, and similarly for L_l. For example, S_1 and S_2 are the diurnal and semidiurnal solar tides, respectively. The tides include both standing $(s = 0)$ and migratory $(s = 1, 2, 3\ldots)$ components.

Each tide consists of a superposition of zonal wave numbers. For example,

$$S_l = \sum_{s=0}^{\infty} S_l^s . \tag{34.57}$$

Haurwitz (1956) summarized data on $S_2(p_0)$, based on 296 stations, as shown in Fig. 34.6. There are two main families, $S_2^2(p_0)$ and $S_2^0(p_0)$. Here $S_2^2(p_0)$ moves westward with the sun. It has a maximum amplitude of about 1.2 mb on the Equator, as can be seen in Fig. 34.6 a. At a given station, p_0 is greatest at 9:44 am and pm (local time). $S_2^0(p_0)$ is

n	*s*	*First Class To West, hours*	*First Class To East, hours*	*Second Class Only to West, days*
1	1	13.76	39.34	1.21
2	1	10.92	14.50	5.37
	2	11.80	18.10	1.64
3	1	9.11	10.09	8.75
	2	9.23	10.96	3.87
	3	9.63	12.17	2.10
4	1	7.65	7.99	12.78
	2	7.65	8.28	6.11
	3	7.75	8.66	3.79
	4	7.94	9.18	2.56
5	1	6.52	6.67	17.75
	2	6.52	6.79	8.70
	3	6.52	6.95	5.62
	4	6.58	7.24	3.92
	5	6.69	7.49	3.05

Table 34.2: Periods of the free oscillations on the sphere, as computed from theory. Note that the periods of the gravity waves are given in hours, while those of the Rossby waves are given in days. From Phillips (1963).

a family of *standing* oscillations, so that phase angles depend on both longitude and local time. According to Haurwitz (1956), the data are well fit by

$$\begin{aligned} S_2^2(p_0) &\cong [1.23P_2^2(\mu) - 0.182P_4^2(\mu) + \dots]\sin(2t + 2\lambda + 158°) \quad \text{mb} \\ S_2^0(p_0) &\cong 8.5P_2^0(\mu)\sin(2t + 118°) \times (10^{-2}) \quad \text{mb} \end{aligned} \tag{34.58}$$

Here $\mu = \sin\varphi$, $t = 2\pi$ (Greenwich time in hours)/24, longitude is taken to be zero on the Greenwich meridian, and $P_n^2(\mu)$ are the seminormalized associated Legendre a

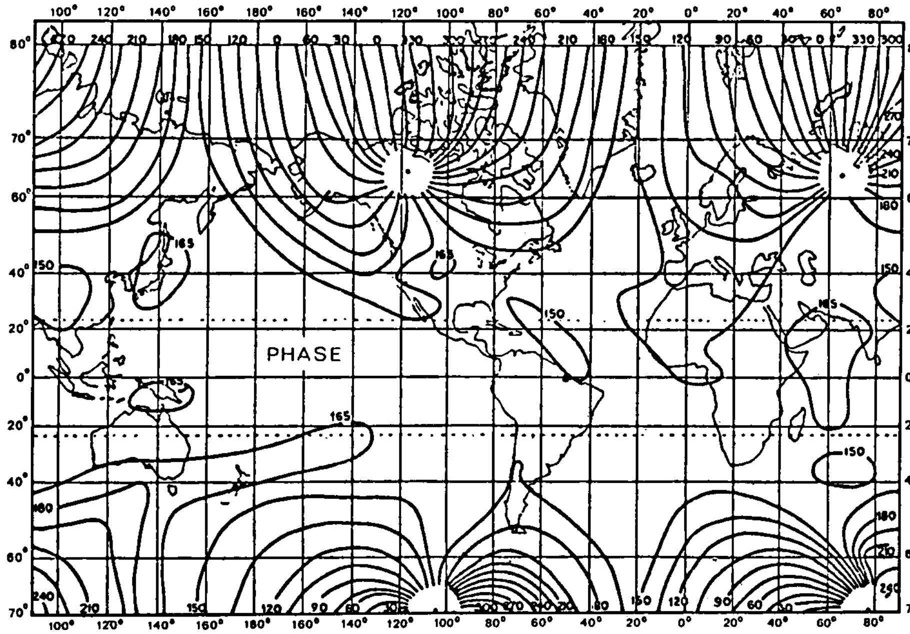

b

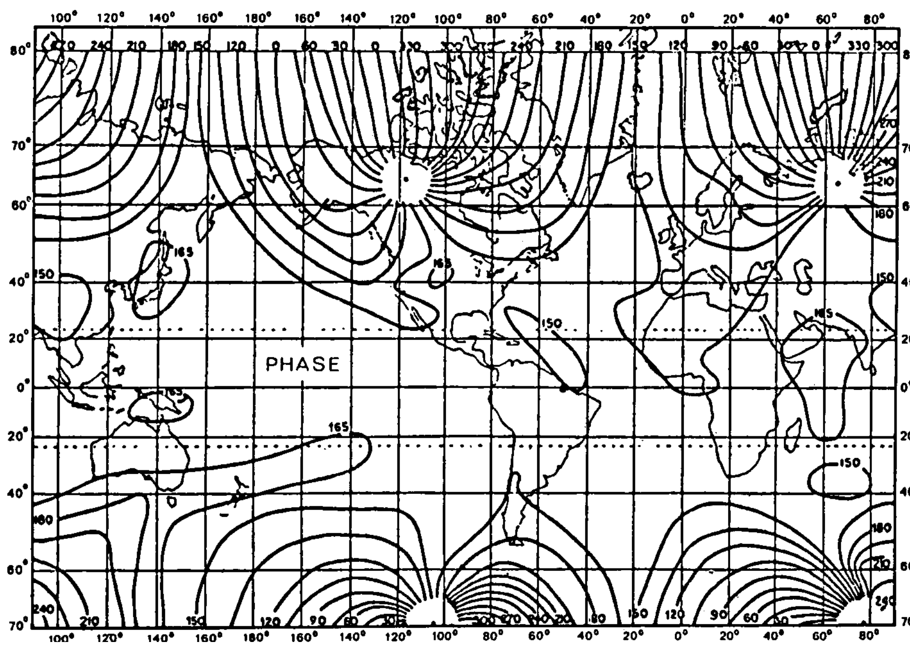

Figure 34.6: a) Observed distribution of the amplitude of S_2 (unit 10^{-2} mb). b) Observed distribution of the phase constant of S_2 in local time. See Eq. (34.58) for the definition of the phase angle. The phase lines come together at nodes where the amplitude of the standing wave is zero. From Haurwitz (1956).

functions with zonal wave number 2. The factor of 158° that appears in the argument of the sine is the "phase constant" plotted in Fig. 34.6 b.

As shown in Fig. 34.7, $S_1(p_0)$ is weaker than $S_2(p_0)$, and is also much less regular over the Earth. Haurwitz first expanded

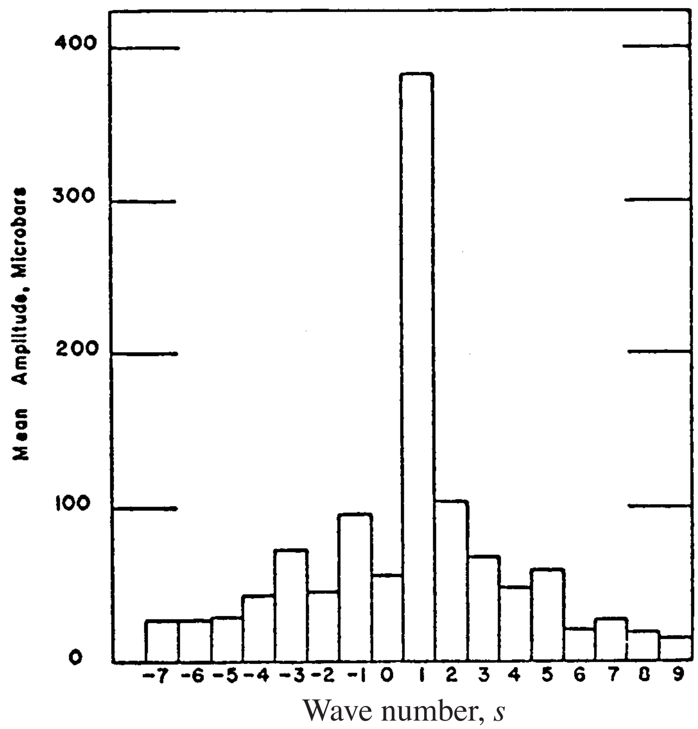

Figure 34.7: Amplitudes of the component waves of the diurnal pressure oscillation. From Haurwitz (1956).

$$S_1(p_0) = a\sin(t' + \alpha) = A\cos t' + B\sin t' , \tag{34.59}$$

where t' is local time. Based on the A's and B's, he determined amplitudes as shown in Fig. 34.7. *Positive wave numbers denote westward propagation*. The major component is $S_1^1(P_0)$. There are many other active modes. They are due to the complicated pattern of heating associated with the distributions of land and sea. The maximum amplitude of $S_1(p_0)$ is about half that of $S_2(p_0)$.

Observations also show the existence of solar tides with shorter periods.

Numerous authors have used upper air data on winds, temperature, and heights to investigate the diurnal and semidiurnal tides, as shown in Fig. 34.8. The dominance of S_2 in the lower troposphere gives way to a dominance of S_1 in the upper troposphere and lower stratosphere. Rocket soundings have revealed strong diurnal and semidiurnal tides between 30 and 60 km as shown in Fig. 34.9. Note the large amplitudes at these altitudes.

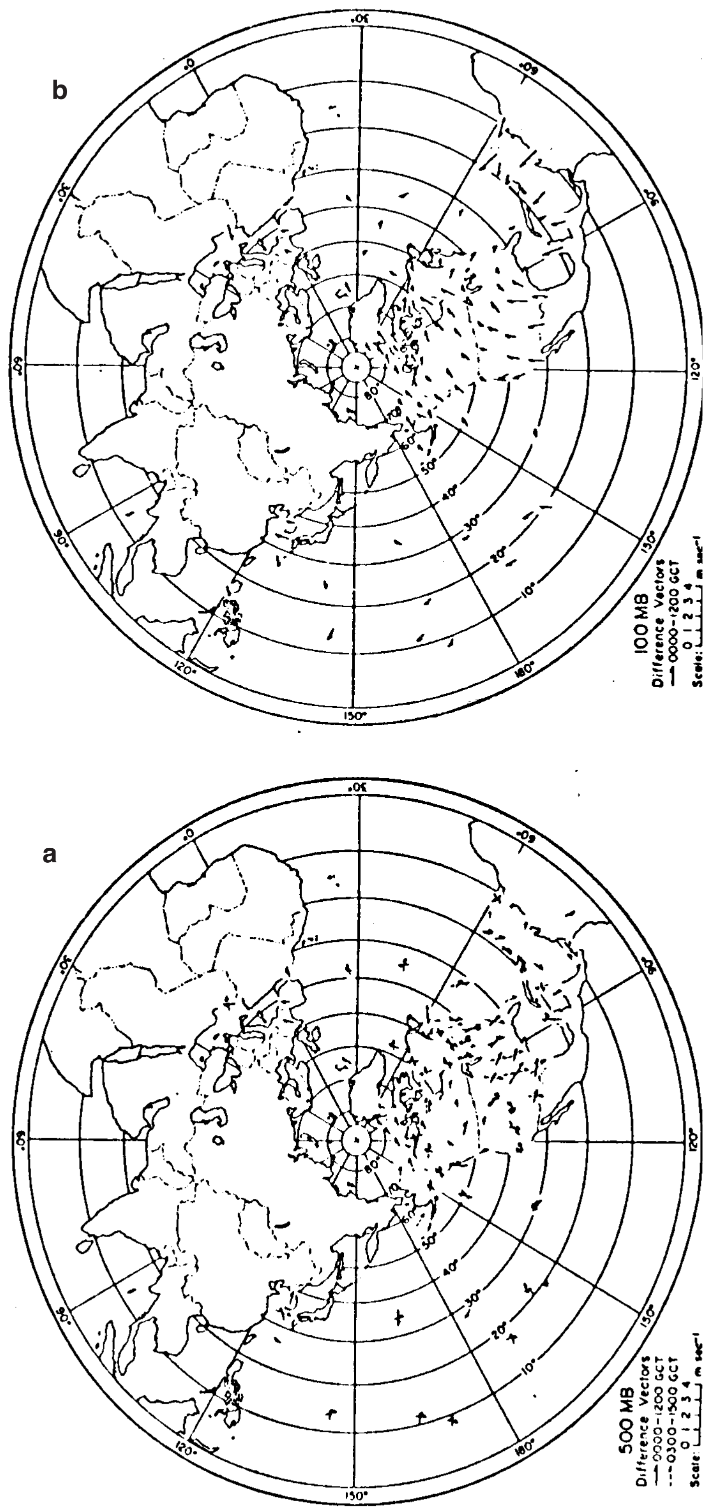

Figure 34.8: a) Annual average 0000 – 1200 GMT (solid) and 0300 – 1500 GMT (dashed) wind differences at 500 mb, plotted in vector form. b) Annual average 0000 – 1200 GMT wind differences at 100 mb plotted in vector form. From Wallace and Hartranft (1969).

In the lower thermosphere (80 - 120 km) the tidal winds attain amplitudes of 20 - 50 m s^{-1}.

Up to now we have been concentrating on the thermally forced solar tides. There are also gravitationally driven lunar tides. As shown in Fig. 34.10,the gravitationally driven lunar tide $L_2(p_0)$ has been detected both in the tropics and in middle latitudes. Its amplitude is measured in μb, reaching about 80 μb on the equator. It exhibits large regional and seasonal irregularities. The major component is $L_2^2(p_0)$, which moves

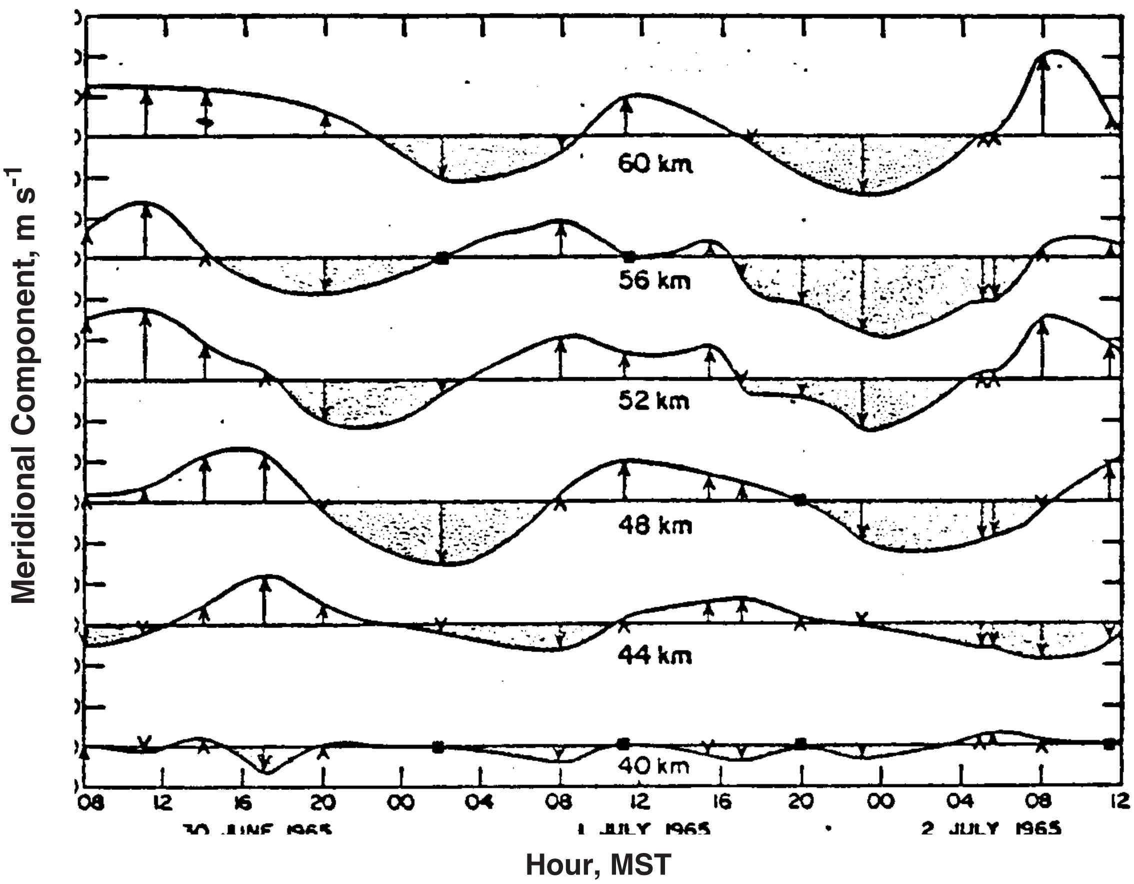

Figure 34.9: Meridional wind components in m s^{-1} averaged over 4 km layers centered at 40, 44, 48, 52, 56 and 60 km. Positive values indicate a south to north flow. From Beyers, Miers, and Reed (1966).

westward with the moon. In the troposphere, the temperature oscillation is on the order of 10^{-2} K, and the wind oscillations are on the order of 10^{-2} m s^{-1}. The gravitationally driven wind oscillations reach 1-2 m s^{-1} near 85-100 km altitude.

Generally speaking, the tides are very well explained by the linear theory. As shown in Fig. 34.11, at high latitudes, the phase is nearly independent of height, suggesting trapped waves. At lower latitudes, the phase changes rapidly with height,

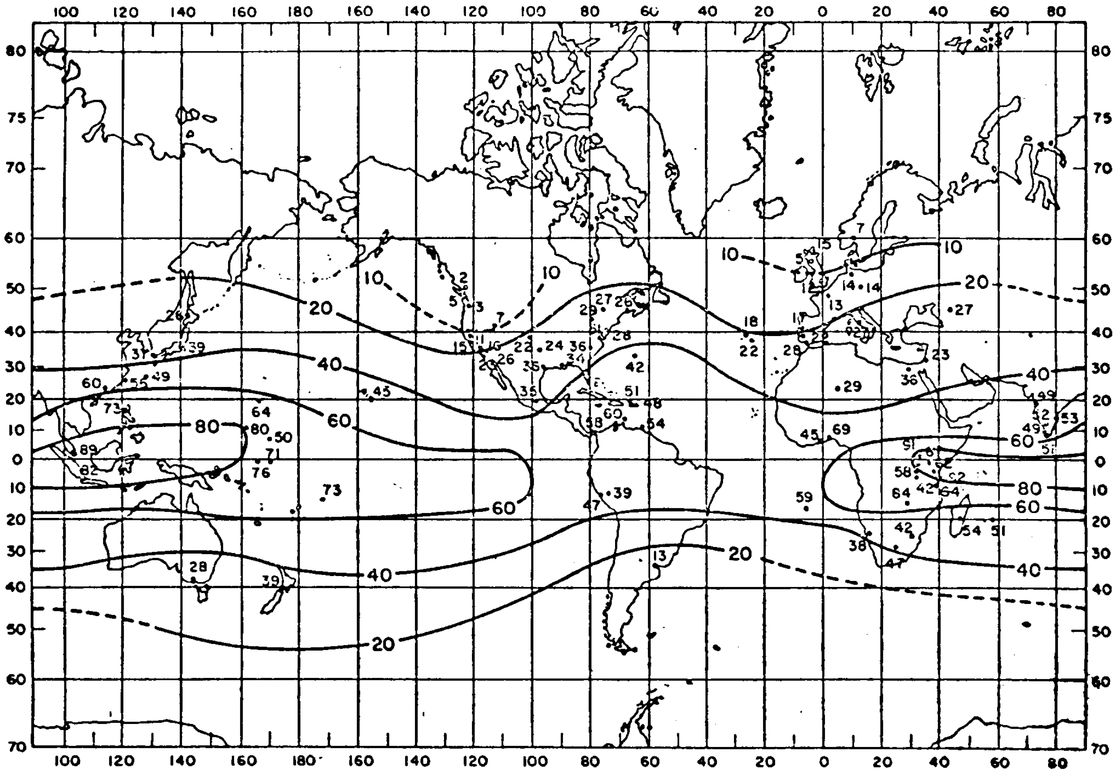

Figure 34.10:Global amplitude distribution of the lunar semidiurnal tide (unit 1 μbar = 10^{-3} mbar). The number at each station dot shows the local amplitude of $L_2(p_0)$. From Haurwitz and Chapman (1967).

indicating vertical propagation of wave energy.

The solar tides are caused by thermal excitation primarily due to absorption of solar radiation by ozone in the stratosphere and water vapor in the troposphere. This heating is *almost independent of the motion of the atmosphere*, and it is periodic. The sun also imposes a periodic gravitational forcing that is completely independent of the motion of the atmosphere. Similarly, gravitational forcing due to the moon is periodic and completely independent of the motion. The theory of the tides seeks to explain how the observed tidal motions are driven by these externally imposed periodic forcings. The fact that the forcing functions for the tides are motion-independent and periodic explains why the theory of the tides is so well developed. It is much more difficult to solve the equations when the forcing (e.g. latent heat release) is dependent on the motion.

Earlier we studied free oscillations. The tides are forced oscillations. For forced oscillations the period (or frequency) and zonal wave number of the forcing are *given*. In contrast, with free oscillations the frequency and zonal wave number of the solution are determined by solving an eigenvalue problem.

For a given σ and s, the LTE,

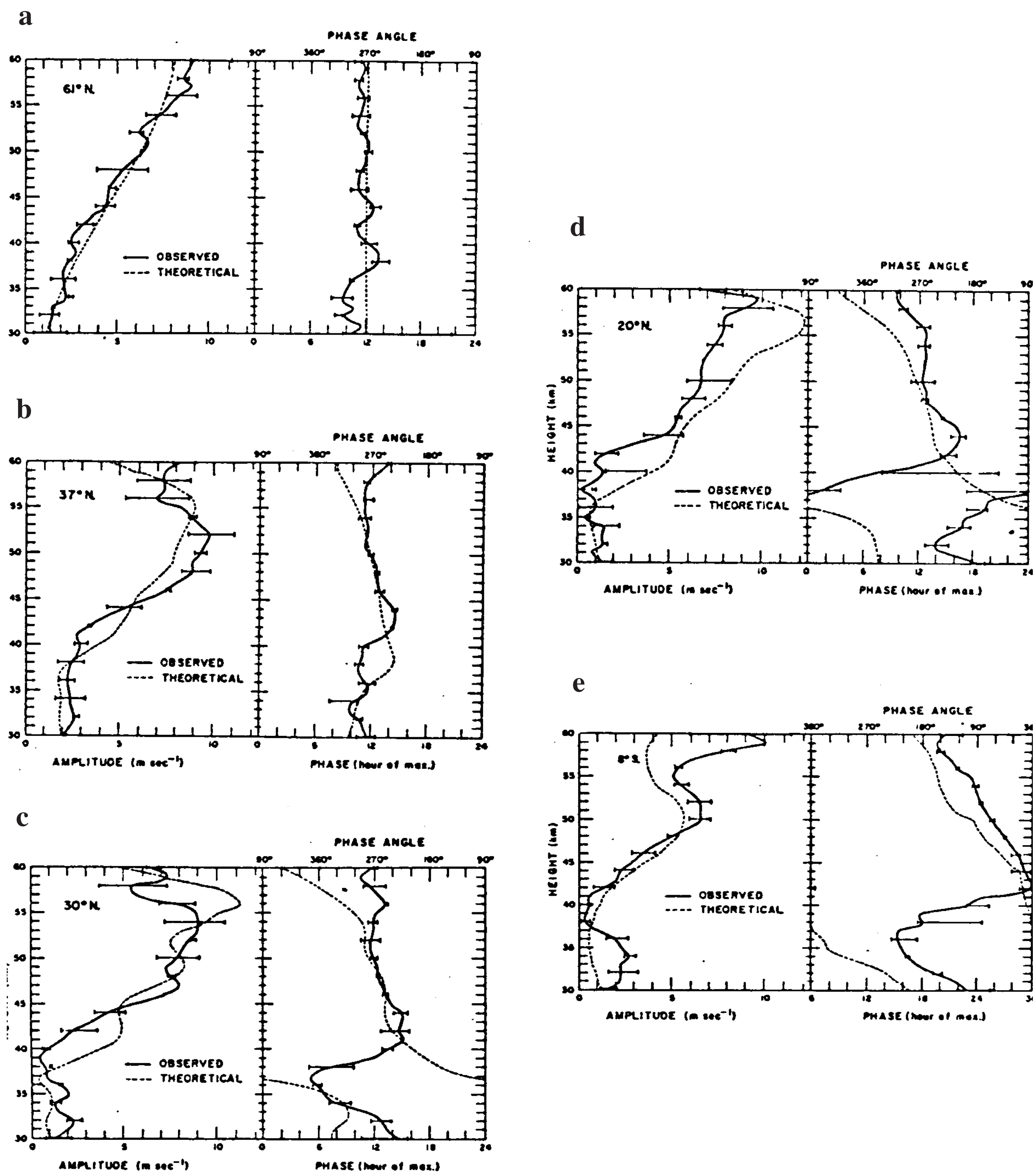

Figure 34.11: a) Amplitude and phase of diurnal variation of meridional wind component at 61° N. The phase angle, in accordance with usual convention, gives the number of degrees in advance of origin (chosen as midnight) that the upcrossing of the sine curve occurs; maximum (max). b) Same as (a) for 37° N. c) Same as (a) for 30° N. d) Same as (a) for 20° N. e) Same as (a) for 8° S. From Reed (1969).

$$\frac{d}{d\mu}\left(\frac{1-\mu^2}{\nu^2-\mu^2}\frac{d\Theta_n^{\sigma,s}}{d\mu}\right) - \frac{1}{\nu^2-\mu^2}\left(\frac{s}{\nu}\frac{\nu^2+\mu^2}{\nu^2-\mu^2}+\frac{s^2}{1-\mu^2}\right)\Theta_n^{\sigma,s} + \frac{4\Omega^2 a^2}{gh_n}\Theta_n^{\sigma,s} = 0 , \qquad (34.60)$$

will yield a generally infinite set of eigenvalues h_n and Hough functions, $\Theta_n^{\sigma,s}$. A method for solving the LTE for the case of forced oscillations was worked out by Hough (1898), who showed that the solutions of the LTE, i.e. the functions named for him, can be expanded in a series of associated Legendre functions. The vertical structure of each eigensolution is determined by solving the vertical structure equation

$$\frac{d^2}{dp^2}W_n^{\sigma,s} + \frac{S_p(p)}{gh_n}W_n^{\sigma,s} = \frac{-R}{c_p g h_n}\left(\frac{J_n^{\sigma,s}}{p}\right) , \qquad (34.61)$$

using with the boundary condition

$$\frac{dW_n^{\sigma,s}}{dp} - \frac{R\bar{T}_0}{p_0 g h_n}W_n^{\sigma,s} = \frac{i\sigma}{gh_n}G_n^{\sigma,s} \text{ at } p = p_0 . \qquad (34.62)$$

Recall that J is the heating and G is the gravitational potential, and that these are both regarded as known here. When the excitation is thermal, we need to know the vertical profile of J_n. If the heating is confined to certain levels (the ozone layer, for instance), the solution is basically the unforced (homogeneous) solution away from those levels.

The solution procedure is shown in Fig. 34.12. Note that the basic logic of this

$$\begin{array}{c} \text{Given } \sigma, s \\ \text{of excitation} \end{array} \xrightarrow{(34.60)} \text{infinite set of } h_n \text{ and } \Theta_n^{\sigma,s} \xrightarrow[\text{plus knowledge of } J_n^{\sigma,s},\ G_n^{\sigma,s}, \text{ and } S_p(p)]{(34.61)} W_n^{\sigma,s}$$

Figure 34.12: The solution procedure for forced oscillations. The frequency is given in the specification of the forcing.

procedure is quite different from that used to study free oscillations.

Extensive tabulations of $\Theta_n^{\sigma,s}$ and h_n are available for various σ and s. Examples are shown in Table 34.3.

To solve the vertical structure equation, (34.61), it is useful to make a change of variables:

Solar semidiurnal tide S_2^2: $1 = 2, m = 2, \sigma = 1.4544 \times 10^{-4}\ \text{sec}^{-1}, f = 0.99727$	
Wave type $n = 4$.	$h_{2,2}^2 = 7.85\ \text{km}$ $\Theta_{2,2}^2 = P_2^2 - 0.339P_4^2 + \ldots$
Wave type $n = 4$:	$h_{2,4}^2 = 2.11\ \text{km}$ $\Theta_{2,4}^2 = 0.202P_2^2 + P_4^2 - 0.819P_6^2 + 0.24P_8^2 - \ldots$
Lunar semidiurnal tideL_2^2: $1 = 2, m = 2, \sigma = 1.4052 \times 10^{-4}\ \text{sec}^{-1}, f = 0.96350$	
Wave type $n = 2$:	$h_{2,2}^2 = 7.07\ \text{km}$ $\Theta_{2,2}^2 = P_2^2 - 0.375P_4^2 + \ldots$
Wave type $n = 4$:	$h_{2,4}^2 = 1.85\ \text{km}$ $\Theta_{2,4}^2 = 0.227P_2^2 + P_4^2 - 0.951P_6^2 + 0.32P_8^2 - \ldots$
Solar ter-diurnal tide S_3^3: $1 = 3, m = 3, \sigma = 2.1817 \times 10^{-4}\ \text{sec}^{-1}, f = 1.4959$	
Wave type $n = 3$:	$h_{3,3}^3 = 12.89\ \text{km}$ $\Theta_{3,3}^3 = P_3^3 - 0.105P_5^3 + \ldots$
Wave type $n = 4$:	$h_{3,4}^3 = 7.66\ \text{km}$ $\Theta_{3,4}^3 = P_4^3 - 0.164P_6^3 + \ldots$

Table 34.3: Equivalent depths and Hough's functions for a few important wave types. Computed for the terrestrial constant $\varepsilon h^{-1} = 1.1349 \times 10^{-2}\ \text{km}^{-1}$. Terms in the Hough's functions with coefficients les than 0.1 are omitted. After Siebert (1961). From Craig (1965).

$$\left.\begin{aligned} Z &\equiv ln\left(\frac{p_0}{p}\right) = -ln\left(\frac{p}{p_0}\right) \\ W_n &\equiv -\gamma p e^{\frac{Z}{2}} Y_n = -\gamma p_0 e^{-\frac{Z}{2}} Y_n \end{aligned}\right\} . \tag{34.63}$$

Here $\gamma \equiv \frac{c_p}{c_v}$. Note that Z is non-dimensional. For an isothermal atmosphere, we can show that $dz = \frac{RT}{g}dZ$. We can thus interpret Z as a kind of non-dimensional height. Using (34.63), we can rewrite (34.61) as

$$\frac{d^2 Y_n}{dZ^2} - \frac{1}{4}\left[1 - \frac{4}{h_n}\left(\kappa H + \frac{dH}{dZ}\right)\right] Y_n = \frac{\kappa J_n}{\gamma g h_n} e^{-\frac{Z}{2}} , \tag{34.64}$$

where $\kappa \equiv \frac{R}{c_p}$, and $H \equiv \frac{RT}{g}$. The advantage of (34.64) over (34.61) is that whereas p appears explicitly in (34.61), Z does not appear explicitly in (34.64). This makes (34.64) easier to handle mathematically.

With the Z coordinate, the lower boundary condition becomes

$$\frac{dY_n}{dZ} + \left(\frac{H}{h_n} - \frac{1}{2}\right) Y_n = \frac{i\sigma}{\gamma g h_n} G_n \ \ at \ \ Z = 0 . \tag{34.65}$$

The upper boundary condition is that the kinetic energy density remains bounded as $Z \to \infty$. It can be shown that this implies that the Y_n remain bounded as $Z \to \infty$. In some cases this condition is replaced by a radiation condition that requires upward propagation of energy.

Let

$$\lambda^2 \equiv \frac{1}{4}\left[1 - \frac{4}{h_n}\left(\kappa H + \frac{dH}{dZ}\right)\right] . \tag{34.66}$$

Note that for an isothermal atmosphere $\lambda^2 = \text{constant}$. The solutions of the homogeneous equation are exponential for $\lambda^2 > 0$, i.e.

$$Y_n \sim Ae^{\lambda Z} + Be^{-\lambda Z} , \tag{34.67}$$

and wave-like for $\lambda^2 < 0$, i.e.

$$Y_n \sim Ae^{i\lambda Z} + Be^{-i\lambda Z} \quad \text{for} \quad \lambda^2 < 0 \,, \tag{34.68}$$

For $\lambda^2 > 0$, the exponential solutions are of the "external" type (no nodes in *Z*), and there is no vertical energy propagation, so that forcing produces effects only close to the levels of excitation. When $\lambda^2 < 0$, the solution is of the "internal" type (there *are* nodes in *Z*) and vertical energy propagation does occur, so that forcing can produce effects far from the level where it occurs. For internal modes, the vertical wavelength is essentially $\frac{2\pi}{|\lambda|}$.

The upper boundary condition requires $A = 0$ for the external modes, and $B = 0$ for the internal modes. The latter is the radiation condition.

Ever since the time of Laplace a puzzling question had been recognized: *Why is* $S_2(p_0)$ *stronger than* $S_1(p_0)$? It seems intuitively that the rising and setting sun should force the diurnal tide more strongly than the semi-diurnal tide, and yet the opposite is observed, at least in terms of the oscillations of the surface pressure. One possible explanation is that $S_2(p_0)$ is forced by the gravitational attraction of the sun. This is plausible because a gravitational tide is expected to have a wave-number 2 structure, as shown in Fig. 34.13.

If the solar gravitational semi-diurnal tide is so strong, however, then we must ask why the lunar semi-diurnal tide is observed to be so weak, given that the Earth's atmosphere experiences a gravitational attraction due to the moon which is 2.2 times stronger than that due to the sun.

On the other hand, if $S_2(p_0)$ is thermally forced, then we would expect S_1 to be even stronger than S_2, because thermal forcing has a structure that (at least superficially) appears to prefer wave number 1 (again, see Fig. 34.13). As already mentioned, however, $S_1(p_0)$ is considerably weaker than $S_2(p_0)$.

Kelvin (1882) suggested an explanation that was accepted for a long time, but ultimately proved to be incorrect: he argued that the semi-diurnal tide is thermally driven and that S_2 is selected by (is stronger than S_1 due to) *resonance*. This could happen if the atmosphere had a *free* oscillation with a period very close to 12 hours. Referring back to Table 5.34.2, we see that the FOFC with $n = 2$, $s = 2$ has a period of 11.8 solar hours. As we have seen, $S_2(p_0)$ has a major contribution from $P_2^2(\mu)$). Many investigators tried to find a realistic $T(p)$ such that the free mode for Θ_2^2 had a period of almost *exactly* 12 hours. As shown in Table 34.3, this requires $h_n = 7.85\ km$. As $T(p)$ became better known from observations, the resonance theory became less tenable. It was dealt a major setback when Jacchia and Kopel (1952) showed that the model atmosphere needed to make a strong resonance at 12 solar hours is unrealistically warm (by about 50 K) at

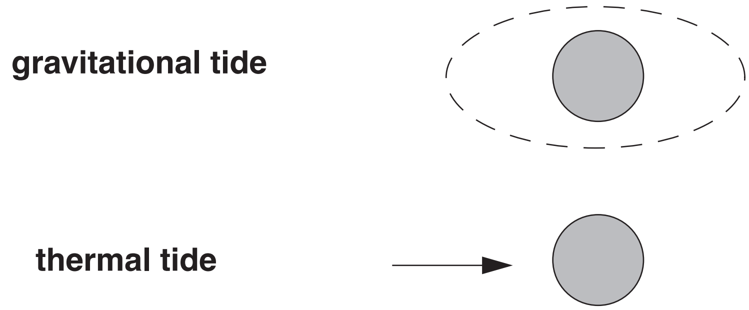

Figure 34.13: Sketch showing the differences between gravitational tides, which are basically "wave number 2," and thermal tides, which are basically "wave number 1." A gravitational tide acts symmetrically on the parts of the planet that are closest to the attracting object and furthest from it. See the problems at the end of the chapter. A thermal tide acts asymmetrically on the part of the planet closest to the radiating object.

the 50 km level. See Fig. 34.14.

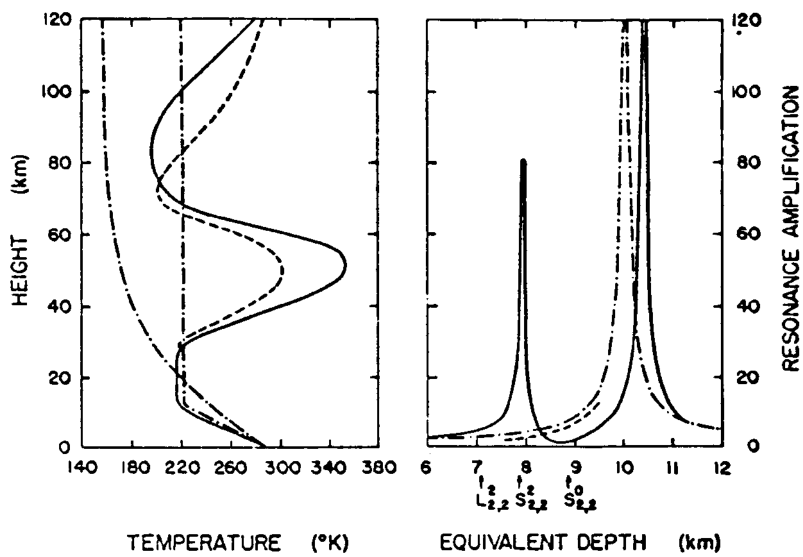

Figure 34.14: Some model atmospheres and the corresponding amplification curves. The solid curves represent an atmosphere devised by Jacchia and Kopal (1952) to give large resonance for $\Theta_{2,2}^{2}$. The dashed curves represent an atmosphere consistent with some early rocket results (computed by Jacchia and Kopal). The dashed-dot curves represent a simple two-layer atmosphere and a mathematical model of Siebert, the resonance curve (computed by Siebert, 1961) being essentially the same for both. (After Siebert, 1961). From Craig

As the resonance theory failed, the question remained: Why is $S_2 \gg S_1$? The explanation came from two directions. First, improved understanding of the heating profile led to larger predicted amplitudes for $S_2(p_0)$. When Siebert (1961) included the effects of solar warming due to tropospheric water vapor, he obtained an amplitude for $S_2(p_0)$ that was about 1/3 that observed. When Butler and Small (1963) included the solar warming due to ozone absorption in the stratosphere, they obtained an amplitude for $S_2(p_0)$ that was about 2/3 that observed.

The second advance was the simultaneous and independent discovery of negative equivalent depths for S_1^1 by Kato (1966) and Lindzen (1966). Three examples are shown in Table 5.34.4. The negative eigenvalues corresponded to previously overlooked solutions of the LTE. From (34.66), we see that small positive h_n's make $\lambda^2(Z)$ large

positive h_n's for $\Theta_n^{\nu=1,\, s=1}$		negative h_n's for $\Theta_n^{\nu=1,\, s=1}$	
n=1	h_1=0.69 km	n=-2	h_{-2}=-12.27 km
n=3	h_3=0.12 km	n=-4	h_{-4}=-1.76 km
n=5	h_5=0.048 km	n=-6	h_{-6}=-0.64 km

Table 34.4: Examples of positive and negative equivalent depths.

and negative, so that although vertical propagation does occur the vertical wavelengths are very small. Such modes have large vertical gradients and so are easily dissipated. Negative h_n's make $\lambda^2(Z)$ positive, so that *the corresponding waves do not propagate vertically*. For these reasons, the S_1 modes excited by ozone absorption *do not reach the ground*, although they can propagate to higher levels. This is now accepted as the reason why $S_1(p_0)$ is much weaker than $S_2(p_0)$.

References and Bibliography

Beyers, N. J., B. T. Miers, and R. J. Reed, 1966: Diurnal tidal motions near the stratopause during 48 hours at White Sands Missile Range. *J. Atmos. Sci.*, **23**, 325-333.

Craig, R. A., 1965: *The Upper Atmosphere. Meteorology and Physics*. Academic Press, 509.

Eliassen, E., and B. Machenhauer, 1965: A study of the fluctuations of the atmospheric planetary flow patterns represented by spherical harmonics. *Tellus*, **17**, 220-238.

Haurwitz, B., 1937: The oscillations of the atmosphere. *Gerlands Beitrage zur Geophysik*, **51**, 195-233.

Haurwitz, B., 1956: The geographical distribution of the solar semidiurnal pressure oscillation. *Meteor. Papers*, New York Univ., 2, No. 5, 36 pp.

Haurwitz, B., and S. Chapman, 1967: Lunar air tide. *Nature*, **213**, 9-13.

Hough, S. S., 1898: On the application of harmonic analysis to the dynamical theory of the tides. Part II. On the general integration of Laplace's dynamical equations. *Phil. Trans. Roy. Soc. London*, **A191**, 139-185.

Hsu, H.-H., and B. J. Hoskins, 1989: Tidal fluctuations as seen in ECMWF data. *Q. J. R. Meteorol. Soc.*, **115,** 247-264.

Jacchia, L. G., and Z. Kopal, 1951: Atmospheric oscillations and the temperature of the upper atmosphere. *J. Meteorol.*, **9**, 13-23.

Kato, S., 1966: Diurnal atmospheric oscillation, 1. Eigenvalues and Hough functions. *J. Geophys. Res.*, **71**, 3201-3209.

Kato, S., 1966: Diurnal atmospheric oscillation, 2. Thermal excitation in the upper atmosphere. *J. Geophys. Res.*, **71**, 3211-3214.

Laplace, P. S., 1832: *Méchanique Céleste*, 4 vols, (Translated by N. Bowditch), Boston. The relevant section is Part I, Book IV, Section 3, p. 543.

Lindzen, R. S., 1966: On the theory of the diurnal tide. *Mon. Wea. Rev.*, **94**, 295-301.

Longuet-Higgins, M. S., 1968: The eigenfunctions of Laplace's tidal equations over a sphere. *Phil. Trans. Roy. Soc. London*, **A262**, 511-607.

Madden, R. A., and P. R. Julian, 1972: Further evidence of global-scale 5-day pressure waves. *J. Atmos. Sci.*, **29**, 1464-1469.

Madden, R. A., and P. R. Julian, 1972: Description of global scale circulation cells in the tropics with a 40-50 day period. *J. Atmos. Sci.,* **29,** 1109-1123.

Reed, R. J., and M. J. Oard, 1969: A comparison of observed and theoretical diurnal tidal motions between 30 and 60 kilometers. *Mon. Wea. Rev.*, **97**, 456-459.

Wallace, J. M., and F. R. Hartranft, 1969: Diurnal wind variations, surface to 30 kilometers. *Mon. Wea. Rev.*, **97**, 446-455.